https://doi.org/10.48048/tis.2023.6736

Artificial Neural Network Model to Predict Filtrate Invasion of Nanoparticle-Based Drilling Fluids

Moamen Gasser[1], Ahmed Naguib[1], Mostafa Magdy Abdelhafiz[1], Sarah Ahmed Elnekhaily[2] and Omar Mahmoud[1,*]

[1]Department of Petroleum Engineering, Faculty of Engineering and Technology, Future University in Egypt, Cairo 11835, Egypt
[2]Department of Metallurgical and Materials Engineering, Faculty of Petroleum and Mining Engineering, Suez University, Suez 43512, Egypt

([*]Corresponding author's e-mail: omar.saad@fue.edu.eg)

Received: 13 February 2023, Revised: 19 February 2023, Accepted: 20 February 2023, Published: 8 March 2023

Abstract

Mud filtrate invasion is a vital parameter that should be optimized during drilling for oil and gas to reduce formation damage. Nanoparticles (NPs) have shown promising filtrate loss mitigation when used as drilling fluid (mud) additives in numerous recent studies. Modeling the influence of NPs can fasten the process of selecting their optimum type, size, concentration, etc. to meet the drilling conditions. In this study, a model was developed, using artificial neural network (ANN), to predict the filtrate invasion of nano-based mud under wide range of pressures and temperatures up to 500 psi and 350 °F, respectively. A total of 2,863 data points were used in the development of the model (806 data points were collected form conducted experiments and the rest were collected form the literature). Seven different types of NPs with size and concentration ranges from 15 to 50 nm and 0 to 2.5 wt%, respectively, had been included in the model to ensure universality. The dataset was divided into 70 % for training and 30 % for validation. A total of 6,750 different combinations for the model's hyperparameters were evaluated to determine the optimum combination. The N-encoded method was used to convert the categorical data into numerical values. The model was evaluated through calculating the statistical parameters. The developed ANN-model proofed to be efficient in predicting the filtrate invasion at different pressures and temperatures with an average absolute relative error (AARE) of less than 0.5 % and a coefficient of determination (R^2) of more than 0.99 for the overall data. The ANN-model covers wide range of pressures, temperatures as well as various NPs' types, concentrations, and sizes, which confirms its useability and coverability.

Keywords: Drilling fluids, Nanoparticles, Mud filtrate invasion, Artificial neural networks, Modeling

Introduction

Drilling oil and gas wells usually requires drilling fluid (mud) that can ensure higher hydrostatic pressures. Drilling such reservoirs at elevated pressures and temperature is challenging. Maintaining the desired characteristics of the drilling mud while taking into consideration the environmental impact has been the goal of numerous studies. Mud filtrate invasion into formations is a vital parameter that can damage the formation and should be mitigated. Different eco-friendly additives had been investigated to improve the properties of drilling fluids, such as henna-leaf extracts and hibiscus-leaf extracts [1], date pit [2], and glass beads [3]. Others, like nanoparticles (NPs) had also been examined as a promising solution for the abovementioned dilemma [4-7].

Iron oxide (Fe_2O_3) and magnetite (Fe_3O_4) NPs decreased the amount of filtrate invasion and enhanced the rheology of bentonite water-based mud (WBM) when used at both high pressure/high temperature (HPHT) and low pressure/low temperature (LPLT) conditions [8-10]. The influence of a synthesized iron oxide NPs on KCl-polymer WBM had also been investigated [11]. Although the addition of silica (SiO_2) NPs showed a complex effect on the rheological properties of mud [10,12], it decreased the filtration invasion of KCl-polymer and bentonite WBM [10,12-14]. Additionally, titanium dioxide (TiO_2) NPs and TiO_2-bentonite nanocomposite reduced the filtration volume of WBM when utilized at HPHT and LPLT [15,16].

The effect of aluminum oxide (Al_2O_3) and copper oxide (CuO) NPs on the WBM performance was the goal of several investigations [17-21]. Adding Al_2O_3 NPs improved both the filtration and rheological

properties of WBM [17,19]. On the other hand, CuO NPs showed improvement in the filtration behavior at longer durations (up to 90 min) when compared to the base fluid with no-NPs [21].

Adding mixture of zinc oxide (ZnO) and CuO NPs in addition to different polymers to WBM showed promising filtration performance at small NPs' concentration [22]. Furthermore, ZnO and magnesium oxide (MgO) NPs showed high capabilities to improve the rheological and filtration properties of WBM at both HPHT and LPLT conditions [16,17,23]. Other NPs like yttrium oxide (Y_2O_3), graphene oxide, carbon, multi wall carbon nanotubes had also been examined as promising drilling mud property modifiers [24-31]. The type and characteristics of mud additives affects its behavior, which is very crucial to the efficiency of the drilling operation. Moreover, the impact of the drilling fluids on the drilled formation [32] and the characteristics of the produced filter cake [33-35] is of paramount importance.

Despite the effectiveness of the experimental studies, artificial intelligence and machine learning techniques are increasingly used in different applications [36,37] among them are the modeling and predicting complex behavior of drilling fluids [38]. Linear regression, supported victor machine, fuzzy logic and artificial neural network (ANN) were applied in different recent studies [39-41]. ANN is inherently used due to its major benefits despite its larger processing time [42].

ANN was capable of predicting rheological characteristics of the muds using marsh funnel viscosity, solid content, and mud density [43,44]. Furthermore, ANN was used to predict the rheology of bentonite-mud using only marsh funnel viscosity and mud density [45]. In 2019, Golsefatan and Shahbazi [46] introduced an ANN model to predict the effect of NPs on the filtration volume of WBM, which showed promising results. Recently, the rheological parameters of nano-modified drilling fluid were predicted using ANN-models based on NPs characteristics and the composition of the drilling fluid [47].

Density and equivalent circulating density (ECD) of the mud have been the subject of other ANN studies. Ultrasonic measurement techniques and ANN was utilized to predict the density, viscosity, and gel strength depending on the time of signal flight, signal amplitude, and the distance that the signal traveled [48]. Furthermore, an ANN-model was developed to predict the density of oil-based mud using the initial mud density, pressure, and temperature [49]. In the meanwhile, mud weight, surface drill pipe pressure and rate of penetration had been used to determine ECD of WBM using artificial intelligence techniques [50].

ANN consists of 3 or more layers; an input layer, an output layer, and one or more hidden layer(s). Each layer consists of number of neurons and are fully connected with weights as shown in **Figure 1**. ANN learn through a training process in which proper exemplars of the data (training dataset) are given to allow the ANN to detect the patterns and relationships between the data. During the training process another dataset (validating dataset) is used to test the model while in training. After the construction of the model, another dataset (testing dataset) is used to test the model on a completely anonymous dataset [51].

The way ANN training process works is by passing the signals form the neurons of the input layer to the neurons of the next layer. All the signals from the neurons of the prior layer goes to each neuron in the following layer. Inside each neuron, the summation of all the inputs multiplies by the weights carrying them is calculated. If the value of the summation is larger than the value of the bias, then this neuron will produce a signal, but if not, it will not produce any signal. If the neuron transmits a signal, the value of the signal will proceed to the activation function then to the next layer [52].

The power of ANN is that there is no need for pre-assumed mathematical equation to be known before building the model. Also, the capability of maintaining its performance even in the presence of some noisy data. So, when it comes to classifying and predicting problems, ANN provides a very strong and reliable solution [53].

Based on the aforementioned literature survey, one can be clearly stated that: 1) using ANN, as a powerful tool, to build models that can predict the properties of drilling fluids can provide very strong, reliable, and cost-effective predictions, 2) there are a lack in the studies that uses ANN to predict the properties of drilling fluids modified with NPs (only 2 studies were conducted [46] and [47]), 3) the study that using ANN to predict the filtration invasion of NPs-based mud was built on the literature data and only considered 1 type of WBM and 5 types of NPs [46], which opens the door for more comprehensive studies.

The objective of this study is to build a more comprehensive ANN model to predict the filtrate fluid volume of the WBM modified with NPs. In this work, 806 data were obtained through laboratory experiments for 3 types of drilling fluids (bentonite WBM, KCl-polymer WBM, and low solid non-dispersed mud (LSNDM)) modified with 6 types of NPs (SiO_2, TiO_2, Al_2O_3, CuO, MgO, ZnO). Furthermore, additional 2,057 data points were collected from the literature (under a wide range of pressures and temperatures) for the aforementioned types of drilling fluids and NPs in addition to Fe_2O_3 NPs. Both KCl-polymer and NaCl-polymer were categorized under the umbrella of salt-polymer WBM. Based on that, a total of 2,863 data points were filtered and used to build an ANN model to predict the volume of

mud filtrate of nano-modified WBM considering the drilling fluid type, the filtration time, and the NPs' type, size, molecular weight, and concentration.

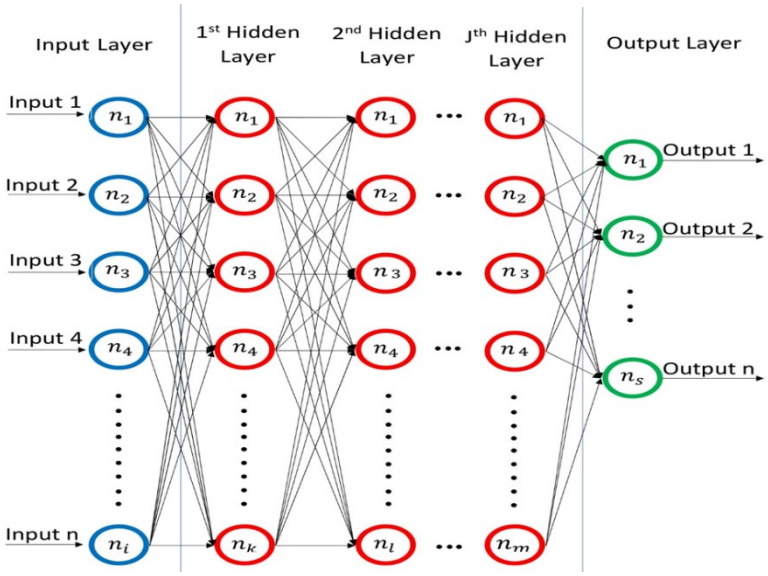

Figure 1 Artificial neural network (ANN) general architecture. ANN consists of 3 or more layers; an input layer, an output layer, and one or more hidden layer(s). Each layer consists of number of neurons and are fully connected with weights.

Methodology

Three types of drilling fluids (bentonite WBM, KCl-polymer WBM, and LSNDM) were prepared using Hamilton Beach 1-spindle mixer (HMD200) and treated by SiO_2, TiO_2, Al_2O_3, CuO, MgO, ZnO NPs with concentrations range from 0.1 to 1 %wt. After that, A standard API filter press was used to measure the amount of filtrate at ambient temperature and 100 Psi differential pressure. The experimental data in additional to the data collected from literature were filtered and prepared to be used in building the model. MATLAB© was used to construct the ANN model. **Figure 2** shows the work scheme of acquiring/preparing the data and building the model.

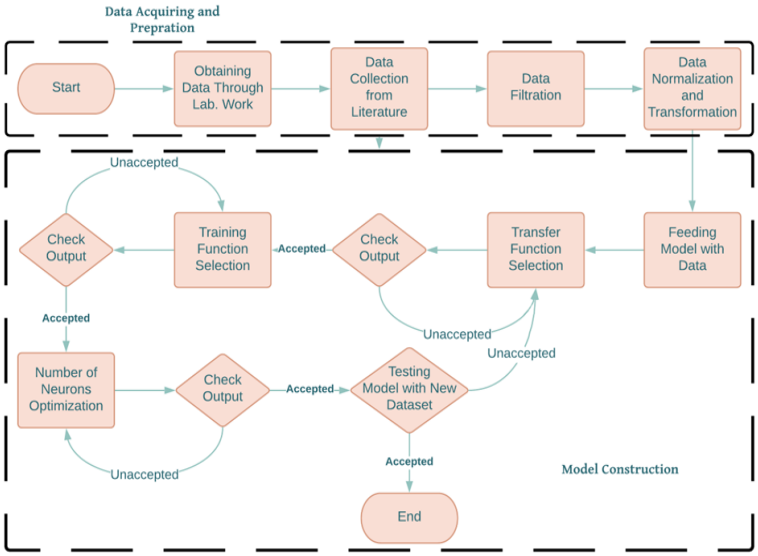

Figure 2 Work scheme of the current study. The work was started by conducting the experimental work to obtain the lab data and collecting the rest from the literature. Then, the data was filtered, normalized, and transformed. After that, the ANN model was fed with the data. Finally, the model was trained, tested, and validated.

Data distribution and preparation

A sample of the used data and their statistical distribution are shown in **Tables 1** and **2**, respectively. Hence, the input contains categorical data (i.e., the drilling fluids and NPs types), N-encoded method was used to convert the categorial data to numerical values as shown in **Table 3**. Firstly, the collected data was filtered, and the noisy data was eliminated for better results. Secondly, the input parameters were normalized to be between 0 and 1 using Eq. (1), while the target parameter (volume of filtrate) was transferred according to Eq. (2) for faster and more efficient training process. Lastly, the data was randomly divided into 2 datasets one for training (70 % of the data) and the other for validating (30 % of the data).

$$X_{i,norm} = \frac{X_i - X_{avg}}{X_{max} - X_{min}} \quad (1)$$

where, i is the number index for each input parameter (drilling fluid type, NPs' type, concentration, molecular weight, and size, and the filtrate time), $X_{i,norm}$ is the normalized value for the input parameter, X_i is the value of the input parameter before normalization, X_{avg} is the average of parameter X_i, X_{max} and X_{min} are the values of the maximum and minimum values of the input parameter X_i.

$$F^T = \ln(F + 1) \quad (2)$$

where, F is the value of filtration volume in *ml* and F^T is the transformed value of the filtrate. **Figures 3** and **4** show the distribution of the values of the filtrate volume before and after the transformation, respectively. **Figure 3** shows the poor distribution of the original filtrate volume data (mainly between 0 and 15 mL). On the other hand, **Figure 4** shows the transformed values of the filtrate volume using Eq. (2), which represents normal distribution and can provide faster and more efficient training process.

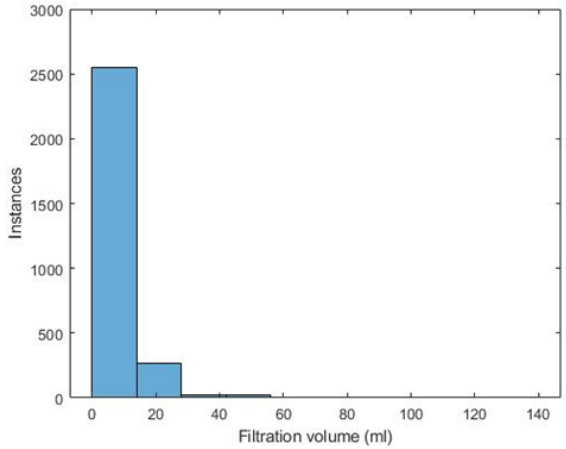

Figure 3 Distribution of the filtrate volume data before transformation.

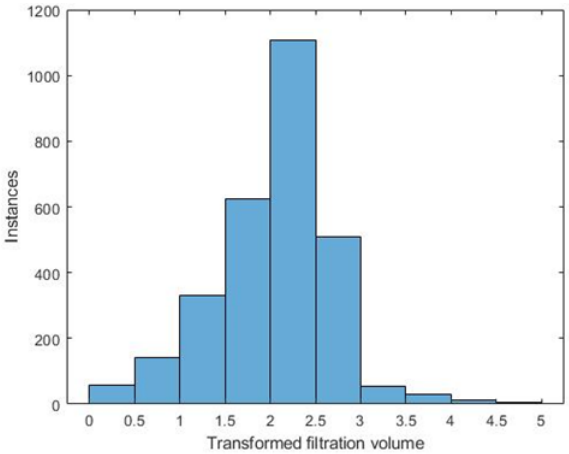

Figure 4 Distribution of the filtrate volume data after transformation.

Model development

A MATLAB© script was developed to go over 6,750 possible combinations (**Figure 5**) of different parameters (the activation function, the training algorithm, and the number of neurons) for 1 hidden layer network (summarized in **Table 4**). Firstly, the transfer function and the training algorithm were determined based on the evaluation of each combination using root mean square error (RMSE) and correlation coefficient (R^2). The combination that gave the lowest RMSE and highest R^2 was chosen. Secondly, the number of neurons in the hidden layer were optimized by plotting the RMSE (**Figure 6**) and R^2 (**Figure 7**). versus a number of neurons between 1:60. As shown in **Figures 6** and **7**, the number of neurons that gave the best performance (the lowest RMSE and highest R^2) was found to be 46.

Table 1 Data sample that shows the different types of the studied WBM, and the different types, sizes, molecular weights, and concentrations of NPs. It also shows the filtrate volumes and the conditions at which they obtained (i. e., pressure, temperature, and time of filtration). Additionally, it shows the category of the collected data (literature or experimental data)

Number	Drilling Fluid Type	NPs' Type	NPs' Size (nm)	NPs' MW (g/mol)	NPs' Conc. (wt%)	T (°F)	P (Psi)	Time (s)	Filtrate Volume (mL)	Experiment or Reference
1	Salt-Polymer	SiO_2	15	60.08	0.1	77	100	1800	16	Exp.
2	Bentonite WBM (BWBM)	-	-	-	-	250	500	1800	17	[10]
3	Low Solids Non-Dispersed (LSNDM)	ZnO	40	81.38	0.5	77	100	3600	14.5	Exp.
4	BWBM	CuO	40	79.545	0.8	ambient	200	600	5.1	[20]
5	Salt-Polymer	ZnO	100	81.38	0.06	250	500	1800	11.8	[23]
6	BWBM	ZnO	40	81.38	1	77	100	5400	18.4	Exp.
7	BWBM	Fe_2O_3	50	159.69	0.3	250	300	60	1.65	[10]
8	Salt-Polymer	Fe_2O_3	11	159.69	0.01	80	100	1800	14.91	[11]
9	LSNDM	CuO	40	79.545	0.3	77	100	900	6	Exp.
10	Salt-Polymer	TiO_2	100	79.866	0.2	150	500	1500	8.4	[16]
11	BWBM	Al_2O_3	35	101.96	0.5	250	500	1800	19.5	[17]
12	LSNDM	TiO_2	50	79.866	0.1	77	100	1500	130	Exp.
13	Salt-Polymer	CuO	40	79.545	1	77	100	900	7	Exp.
14	BWBM	TiO_2	30	79.866	2	75	100	450	6.9	[15]
15	Salt-Polymer	Al_2O_3	40	101.96	0.1	77	100	1200	14.4	Exp.
16	Salt-Polymer	-	-	-	-	250	500	540	6.7	[23]
17	LSNDM	Fe_2O_3	3	159.69	0.5	392	1015	3600	42.4	[8]
18	BWBM	MgO	20	40.3	0.5	250	500	1800	26.5	[17]
19	LSNDM	SiO_2	15	60.08	1	77	100	1200	9.5	Exp.
20	Salt-Polymer	MgO	30	40.3	0.7	77	100	1200	5.9	Exp.
21	BWBM	SiO_2	12	60.08	2.5	300	250	1260	10.6	[10]
22	LSNDM	Al_2O_3	40	101.96	0.7	77	100	300	4	Exp.
23	LSNDM	-	-	-	-	392	1015	600	23.7	[8]
24	LSNDM	MgO	30	40.3	0.3	77	100	60	3	Exp.

Table 2 Statistical distribution of the data

Parameter	Maximum	Minimum	Mean	Median	Mode	SD	Skewness
Drilling Fluid Type	Salt-Polymer WBM, Low Solid Non-Dispersed Mud (LSNDM), and Bentonite Water-Based Mud (BWBM)						
NPs' Type	Ferric oxide (Fe_2O_3), Aluminum oxide (Al_2O_3), Silica oxide (SiO_2), Titanium oxide (TiO_2), Copper oxide (CuO), Magnesium oxide (MgO), and Zinc oxide (ZnO)						
NPs' Concentration (wt%)	2.5	0.001	0.627	0.5	0.5	0.569	1.597
NPs' Molecular Weight (g/mol)	159.69	40.3044	80.757	79.866	60.08	47.289	0.239
NPs' Size (nm)	100	3	34.454	30	50	29.982	0.974
Temperature (°F)	350	77	121.419	80	80	75.787	1.408
Pressure (Psi)	500	100	157.692	100	100	114.435	1.929
Time (sec)	5400	10	1044.025	900	1800	935.568	2.105
Filtrate Volume (mL)	140	0.1	8.473	7.5	9	7.671	6.426

Table 3 Data sample after conversion using N-encoded method. Hence, the input data contains categorical data (i.e., the drilling fluids and NPs types), N-encoded method was used to convert the categorial data to numerical values.

Number	Drilling Fluid Type			NPs' Type							NPs' Size (nm)	NPs' Mw (g/mol)	T (°F)	P (Psi)	Time (s)	Filtrate Volume (mL)	Experiment or Reference
	Salt-Polymer	BWBM	LSNDM	Fe_2O_3	SiO_2	TiO_2	CuO	Al_2O_3	MgO	ZnO							
1	1	0	0	0	0.1	0	0	0	0	0	15	60.08	77	100	1800	16	Exp.
2	0	1	0	0	0	0	0	0	0	0	0	0	250	500	1800	17	[10]
3	0	0	1	0	0	0	0	0	0	0.5	40	81.38	77	100	3600	14.5	Exp.
4	0	1	0	0	0	0	0.8	0	0	0	40	79.545	80	200	600	5.1	[20]
5	1	0	0	0	0	0	0	0	0	0.06	100	81.38	250	500	1800	11.8	[23]
6	0	1	0	0	0	0	0	0	0	1	40	81.38	77	100	5400	18.4	Exp.
7	0	1	0	0.3	0	0	0	0	0	0	50	159.69	250	300	60	1.65	[10]
8	1	0	0	0.01	0	0	0	0	0	0	11	159.69	80	100	1800	14.91	[11]
9	0	0	1	0	0	0	0.3	0	0	0	40	79.545	77	100	900	6	Exp.
10	1	0	0	0	0	0.2	0	0	0	0	100	79.866	150	500	1500	8.4	[16]
11	0	1	0	0	0	0	0	0.5	0	0	35	101.96	250	500	1800	19.5	[17]
12	0	0	1	0	0	0.1	0	0	0	0	50	79.866	77	100	1500	130	Exp.
13	1	0	0	0	0	0	1	0	0	0	40	79.545	77	100	900	7	Exp.
14	0	1	0	0	0	2	0	0	0	0	30	79.866	75	100	450	6.9	[15]
15	1	0	0	0	0	0	0	0.1	0	0	40	101.96	77	100	1200	14.4	Exp.
16	1	0	0	0	0	0	0	0	0	0	0	0	250	500	540	6.7	[23]
17	0	0	1	0.5	0	0	0	0	0	0	3	159.69	392	1015	3600	42.4	[8]
18	0	1	0	0	0	0	0	0	0.5	0	20	40.3	250	500	1800	26.5	[17]
19	0	0	1	0	1	0	0	0	0	0	15	60.08	77	100	1200	9.5	Exp.
20	1	0	0	0	0	0	0	0	0.7	0	30	40.3	77	100	1200	5.9	Exp.
21	0	1	0	0	2.5	0	0	0	0	0	12	60.08	300	250	1260	10.6	[10]
22	0	0	1	0	0	0	0	0.7	0	0	40	101.96	77	100	300	4	Exp.
23	0	0	1	0	0	0	0	0	0	0	0	0	392	1015	600	23.7	[8]
24	0	0	1	0	0	0	0	0	0.3	0	30	40.3	77	100	60	3	Exp.

Table 4 Different combinations for the tested parameters.

Parameter	Range
Training Functions	TRAINBFG, TRAINBR, TRAINCGB, TRAINCGF, TRAINCGP, TRAINGD, TRAINGDM, TRAINGDA, TRAINGDX, TRAINLM, TRAINOSS, TRAINR, TRAINRP, TRAINSCG
Transfer Functions	Logsig, Tansig, Purelin, Relu
Number of Neurons in the Hidden Layer	1:30
Number of Neurons in the Hidden Layer for the Chosen Combination	1:60

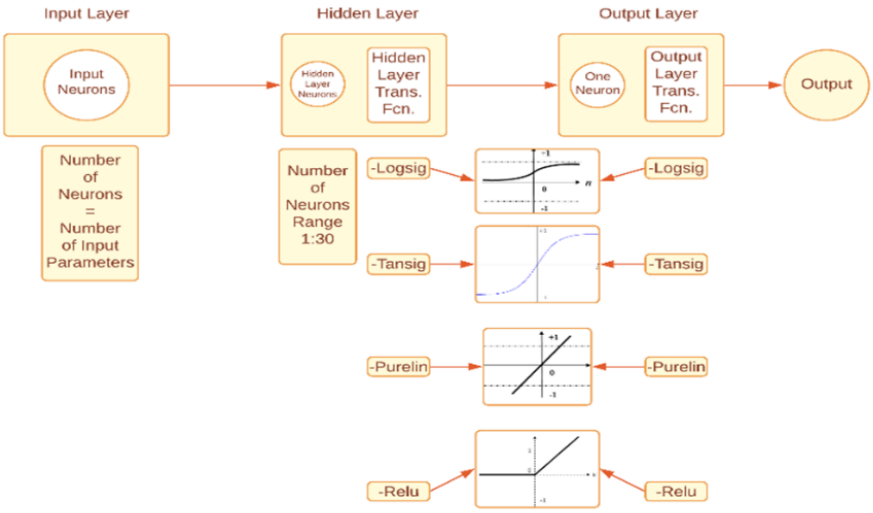

Figure 5 The tested parameters of the model. A MATLAB© script was developed to go over 6,750 possible combinations of different parameters (i.e., the activation function, the training algorithm, and the number of neurons) for 1 hidden layer network.

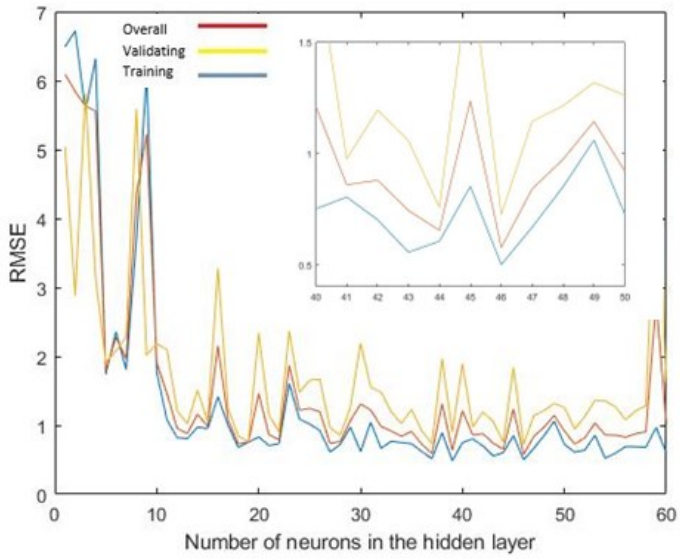

Figure 6 RMSE versus the number of neurons in the hidden layer.

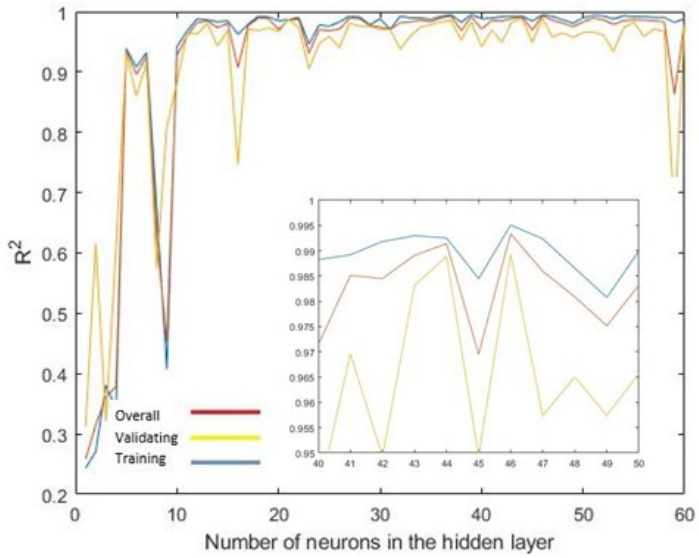

Figure 7 R2 versus the number of neurons in the hidden layer.

Results and discussion

The ANN model was developed to predict the volume of filtrate in mL according to Eq. (3). The number of neurons in the hidden layer was optimized to be 46 according to **Figures 6** and **7**. Levenberg-Marquardt optimization was used as training algorithm. TANSIG and PURELIN were selected to be the hidden and output layers transfer functions, respectively, as shown in **Figure 8**.

$$F = Exp\left[\left[\sum_{i=1}^{N} W_{2i} TANSIG\left(\sum_{j=1}^{J} W_{1j} \times X_j + b_{1i}\right)\right] + b_2\right] - 1 \quad (3)$$

where, *Exp* is the exponential function, *N* is the number of neurons in the hidden layer, W_{2i} is weight of the output layer, *J* is the number of input variables, W_1 is weight of hidden layer, X_j is the normalized input variable (i.e., the drilling fluid type, the NPs' type, concentration, molecular weight, and size, and the pressure, temperature, and filtration time), b_1 is bias of the hidden layer, and b_2 is bias of the output layer. The values of the weights and bias are shown in **Appendixes Tables A1 - A4**.

Furthermore, the model was used to predict the filtration volume then the predicted values were plotted versus the actual values as shown in **Figure 9**. The figure represents the efficiency of the ANN results in relation to targets of training and validation datasets. For an ideal fit, the data points should fall near the line of the unit slope, where the ANN results are equal to the targets. The results indicate that the fit is good for all datasets. Several statistical tests were conducted between the actual and the predicted data to test the model. Average absolute percentage error (ARE), absolute average relative error (AARE), relative deviation (RD), standard deviation (SD), mean square error (MSE), RMSE, R^2, and the ratio between the predicted data to the actual data are used to evaluate the model according to Eqs. (4) - (11).

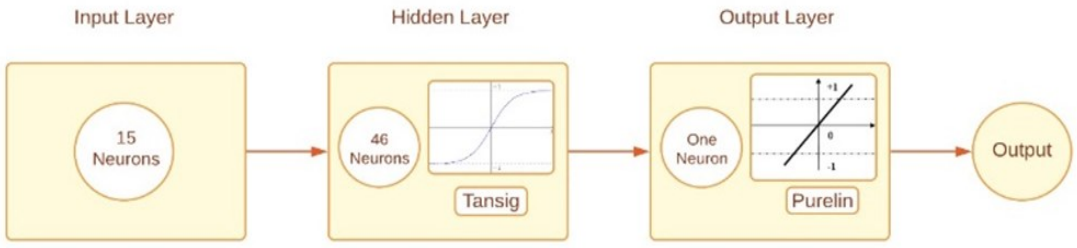

Figure 8 ANN structure for the proposed model. The number of neurons in the hidden layer was optimized to be 46. Levenberg-Marquardt optimization was used as training algorithm. TANSIG and PURELIN were selected to be the hidden and output layers transfer functions, respectively.

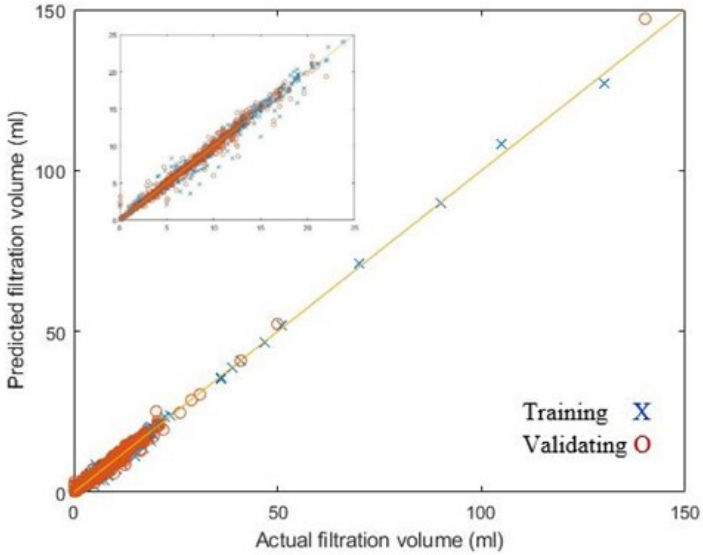

Figure 9 Predicted values of the filtration volume versus the actual values for both training and validating datasets. The results indicate that the fit is good for all datasets. The data points fall near the line of the unit slope, where the ANN results are equal to the targets.

$$ARE = \left(\frac{1}{N} \times \sum_{i=1}^{N} \frac{F^{Predicted} - F^{Actual}}{F^{Actual}}\right) \times 100 \quad (4)$$

$$AARE = \left(\frac{1}{N} \times \sum_{i=1}^{N} \left|\frac{F^{Predicted} - F_i^{Actual}}{F_i^{Actual}}\right|\right) \times 100 \quad (5)$$

$$RD = \frac{F^{Predicted} - F^{Actual}}{F^{Actual}} \times 100 \quad (6)$$

$$SD = \left\{\frac{1}{N-1} \times \sum_{i=1}^{N} \left(\frac{F^{Predicted} - F^{Actual}}{F^{Actual}}\right)^2\right\}^{0.5} \quad (7)$$

$$MSE = \frac{1}{N} \times \sum_{i=1}^{N} (F^{Predicted} - F^{Actual})^2 \quad (8)$$

$$RMSE = \left\{\frac{1}{N} \times \sum_{i=1}^{N} (F^{Predicted} - F^{Actual})^2\right\}^{0.5} \quad (9)$$

$$R^2 = 1 - \frac{\sum_{i=1}^{N} (F^{Predicted} - F^{Actual})^2}{(F_{Actual}^{Mean} - F^{Actual})^2} \quad (10)$$

$$Ratio = \frac{F^{Predicted}}{F^{Actual}} \quad (11)$$

where, N is the number of data points tested, $F^{Predicted}$ is the predicted filtration volume in mL, F^{Actual} is the corresponding actual filtration volume in mL, and F_{Actual}^{Mean} is the average of the actual filtration volume in mL. The aforementioned tests were applied for the training and validating datasets separately to make sure that the model is not overfitted to the training dataset. Furthermore, the overall performance of the model was measured and compared to the results from both datasets as shown in **Figure 10**. The R^2, MSE, RMSE, ARE, AARE, and SD for the overall dataset were 0.9941, 0.3408, 0.5838, 0.0042, 0.0515 and 0.1855, respectively, which shows higher accuracy.

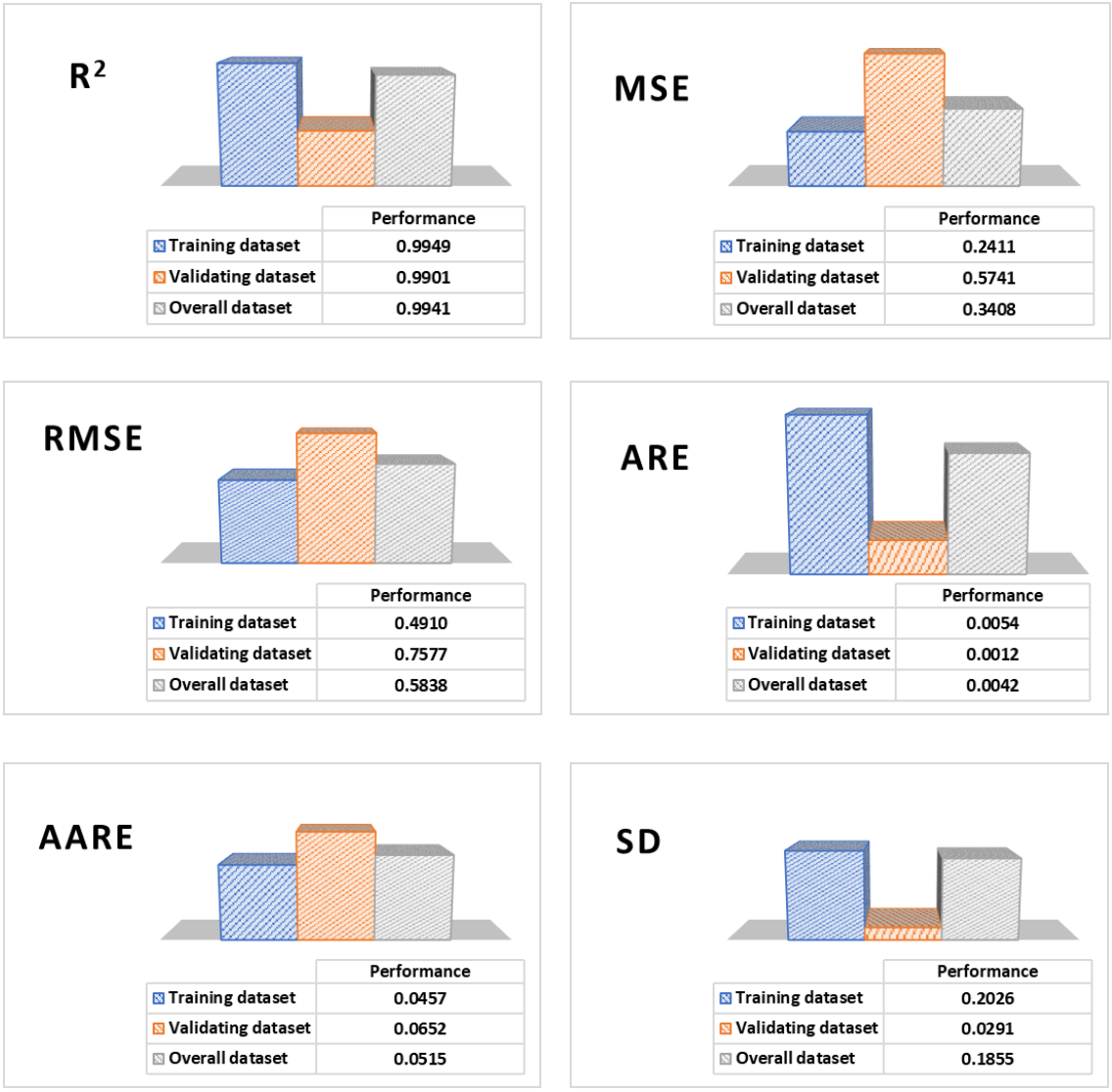

Figure 10 Graphical representation of R^2, RMSE, ARE, MSE, SD, and AARE for training, validating, and overall datasets. R^2, MSE, RMSE, ARE, AARE, and SD for the overall dataset were 0.9941, 0.3408, 0.5838, 0.0042, 0.0515 and 0.1855, respectively.

Moreover, the deviation of the predicted data relative to the actual data was measured in relative deviation (RD) and plotted versus the value of the actual data as shown in **Figure 11**. RD measures the difference between predicted and actual data and gives an illustrative view about the adjacency of actual and model target. The maximum RD were 92.4 and 119 while the minimum RD were −59.1 and −46.8 for the training and validating datasets, respectively, which illustrates the consistency between the actual and predicted filtration volumes. In addition, the ratio between the predicted values to the actual values is presented in **Figure 12**. The average ratio was found to be 1.005 for the training dataset and 1.001 for the validating dataset, which represents an average ratio of 1.004 for the overall dataset.

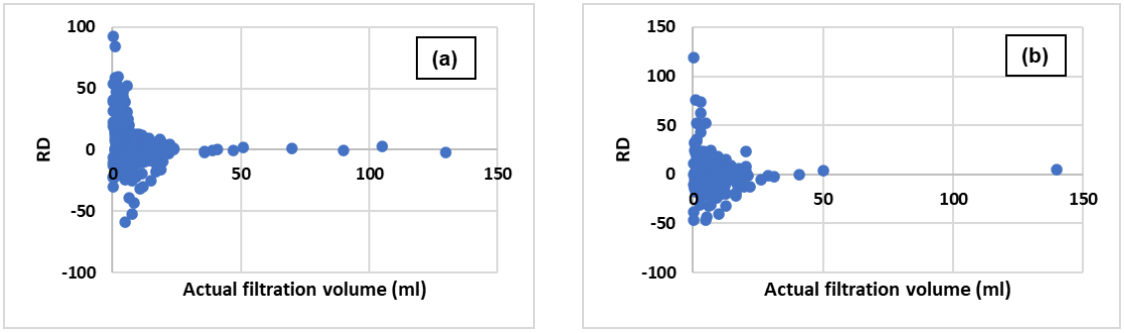

Figure 11 RD versus actual filtration volume for (a) training, and (b) validating datasets. The maximum RD were 92.4 and 119 while the minimum RD were −59.1 and −46.8 for the training and validating datasets, respectively.

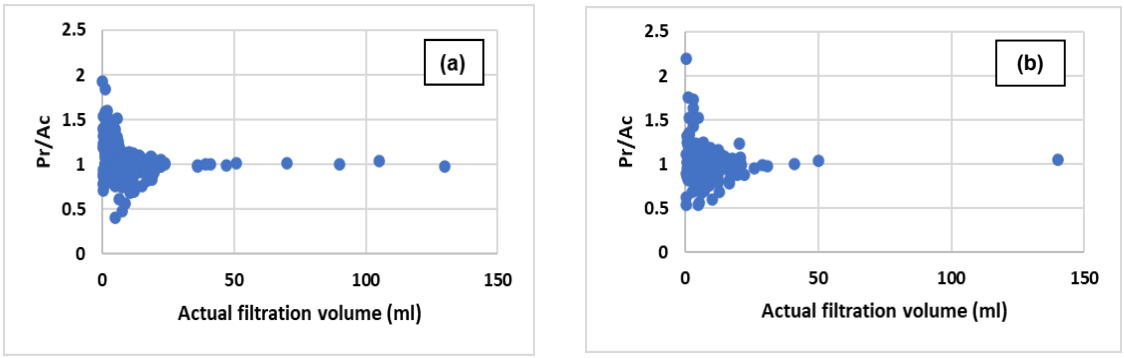

Figure 12 The ratio between the predicted and actual filtration volume versus the actual volume for (a) training, and (b) validating datasets. The average ratio was found to be 1.005 for the training dataset and 1.001 for the validating dataset, which represents an average ratio of 1.004 for the overall dataset.

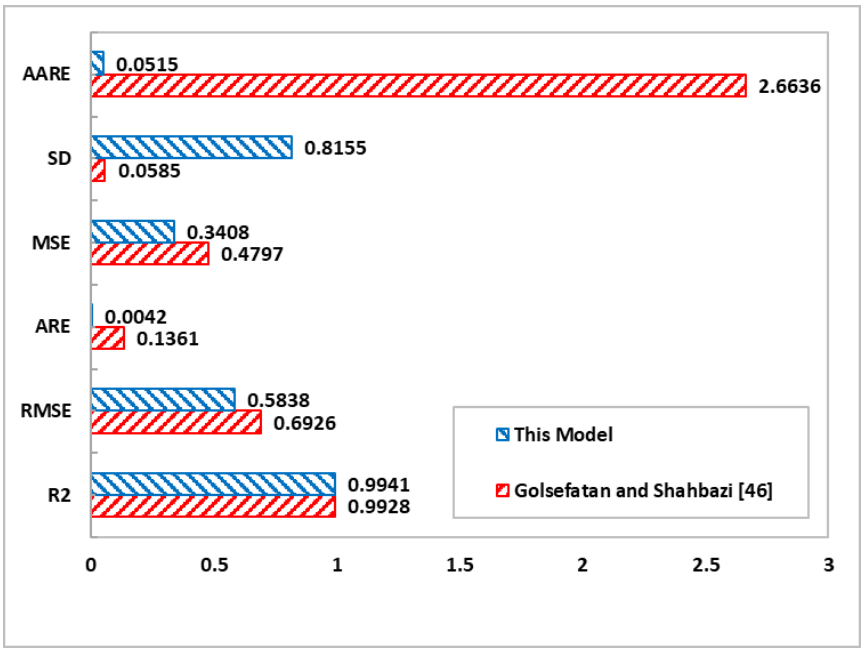

Figure 13 Comparison between the proposed model and the Golsefatan and Shahbazi model based on R^2, RMSE, ARE, MSE, SD, and AARE. The statistical parameters confirm the better accuracy of the newly developed model.

Golsefatan and Shahbazi [46] model was the first attempt to predict the impact of NPs on the filtration volume of WBM, which showed promising results. By comparing the developed model in the current study with the Golsefatan and Shahbazi model, one can conclude that: 1) the newly developed model considers 3 different types of WBM (bentonite WBM, salt-polymer WBM, and low solid non-dispersed mud (LSNDM)); however, the other model only considers the data of KCl-polymer WBM, 2) the number of data points used in the newly developed model are 2,863 for 7 different types of NPs; whereas only 1,003 data points for only 5 types of NPs were used in building the other model, 3) the overall accuracy of the newly developed model is higher compared to that of the Golsefatan and Shahbazi model as shown in **Figure 13**. The R^2, MSE, RMSE, ARE, AARE, and SD for the overall dataset of the Golsefatan and Shahbazi model were 0.9928, 0.4797, 0.6926, 0.1361, 2.6636 and 0.0585, respectively. Whereas the same statistical parameters of the newly developed model were 0.9941, 0.3408, 0.5838, 0.0042, 0.0515 and 0.1855, respectively, which confirms better accuracy.

Conclusions

An ANN-model to predict the volume of filtrate of NPs-based WBM was developed. 2,863 data points were collected from both experimental work and literature, then normalized and transformed, and used in the model training, testing, and validation. Different statistical tests were conducted to evaluate the newly developed model. R^2, MSE, RMSE, ARE, AARE, and SD for the overall dataset were found to be 0.9941, 0.3408, 0.5838, 0.0042, 0.0515 and 0.1855, respectively. RD and the ratio between the predicted to the actual data points were also used to evaluate the model. The ratio between the predicted to the actual values of the filtrate volumes was 1.004 for the overall dataset. The overall model performance was compared to the Golsefatan and Shahbazi model [46], which showed the higher accuracy of the newly developed model in predicting the filtration volume. The developed model presents a very promising solution for the optimization and atomization of the drilling process by directly estimating the filtration volumes of the drilling fluids, which can reduce the hazards and decrease the risk.

Acknowledgements

The authors would like to express their sincere thanks and appreciation to the Future University in Egypt (FUE), Egypt for their continuous encouragement and support.

References

[1] AR Ismail, NMNA Mohd, NF Basir, JO Oseh, I Ismail and SO Blkoor. Improvement of rheological and filtration characteristics of water-based drilling fluids using naturally derived henna leaf and hibiscus leaf extracts. *J. Pet. Explor. Prod. Tech.* 2020; **10**, 3541-56.

[2] JK Adewole and MO Najimu. A study on the effects of date pit-based additive on the performance of water-based drilling fluid. *J. Energ. Resour. Tech.* 2018; **140**, 052903.

[3] A R Ismail, A Aftab, Z H Ibupoto and N Zolkifile. The novel approach for the enhancement of rheological properties of water-based drilling fluids by using multi-walled carbon nanotube, nanosilica and glass beads. *J. Pet. Sci. Eng.* 2016; **139**, 264-75.

[4] A Mady, O Mahmoud and A Dahab. Can nanoparticles improve the characteristics of drilling fluids? *In*: Proceedings of the 13th International Conference on Mining, Metallurgical, and Petroleum Engineering, Suez, Egypt. 2019.

[5] A Mady, O Mahmoud and A Dahab. Nanoparticle-based drilling fluids as promising solutions to enhance drilling performance in Egyptian oil and gas fields. *J. Indust. Sustain. Dev.* 2020; **1**, 24-38.

[6] A Mady, O Mahmoud and A Dahab. Nanoparticles as promising additives to improve the drilling of Egyptian oil and gas fields. *In*: Proceedings of the ASME 39th International Virtual Conference on Ocean, Offshore and Arctic Engineering. Florida, United States, 2020.

[7] A Aftab, M Ali, M Arif, S Panhwar, NMC Saady, EA Al-Khdheeawi, O Mahmoud, AR Ismail, A Keshavarz and S Iglauer. Influence of tailor-made TiO_2/API bentonite nanocomposite on drilling mud performance: Towards enhanced drilling operations. *Appl. Clay Sci.* 2020; **199**, 105862.

[8] MM Barry, Y Jung, JK Lee, TX Phuoc and MK Chyu. Fluid filtration and rheological properties of nanoparticle additive and intercalated clay hybrid bentonite drilling fluids. *J. Pet. Sci. Eng.* 2015; **127**, 338-346.

[9] Z Vryzas, O Mahmoud, HA Nasr-El-Din, V Zaspalis and VC Kelessidis. Incorporation of Fe_3O_4 nanoparticles as drilling fluid additives for improved drilling operations. *In*: Proceedings of the ASME 35th International Conference on Ocean, Offshore and Arctic Engineering, Busan, South Korea. 2016.

[10] Z Vryzas, O Mahmoud, HA Nasr-El-Din and VC Kelessidis. Development and testing of novel drilling fluids using Fe_2O_3 and SiO_2 nanoparticles for enhanced drilling operations. *In*: Proceedings of the International Petroleum Technology Conference, Doha, Qatar. 2015.
[11] MAA Alvi, M Belayneh, S Bandyopadhyay and MW Minde. Effect of iron oxide nanoparticles on the properties of water-based drilling fluids. *Energies* 2020; **13**, 6718.
[12] O Mahmoud, HA Nasr-El-Din, Z Vryzas and VC Kelessidis. Using ferric oxide and silica nanoparticles to develop modified calcium bentonite drilling fluids. *SPE Drill. Compl.* 2018; **33**, 12-26.
[13] AH Salih, TA Elshehabi and HI Bilgesu. Impact of nanomaterials on the rheological and filtration properties of water-based drilling fluids. *In*: Proceedings of the SPE Eastern Regional Meeting, Ohio, United States. 2016.
[14] G Cheraghian, Q Wu, M Mostofi, MC Li, M Afrand and JS Sangwai. Effect of a novel clay/silica nanocomposite on water-based drilling fluids: Improvements in rheological and filtration properties. *Colloids Surf. A Physicochem. Eng. Asp.* 2018; **555**, 339-50.
[15] V Nooripoor, R Nazemi and A Hashemi. Employing nano-sized additives as filtration control agent in water-based drilling fluids: study on barium sulfate, bentonite, surface-modified bentonite, titanium oxide, and silicon oxide. *Energ. Sources A Recovery Util. Environ. Eff.* 2020. https://doi.org/10.1080/15567036.2020.1805049
[16] AA Nizamani, AR Ismail, R Junin, AQ Dayo, AH Tunio, ZH ibupoto and MAM Sidek. Synthesis of titania-bentonite nanocomposite and its applications in water-based drilling fluids. *Chem. Eng. Trans.* 2017; **56**, 949-54.
[17] MT Al-saba, AA Fadhli, A Marafi, A Hussain, F Bander and MFA Dushaishi. Application of nanoparticles in improving rheological properties of water based drilling fluids. *In*: Proceedings of the SPE Kingdom of Saudi Arabia Annual Technical Symposium and Exhibition, Dammam, Saudi Arabia. 2018.
[18] SR Smith, R Rafati, AS Haddad, A Cooper and H Hamidi. Application of aluminium oxide nanoparticles to enhance rheological and filtration properties of water based muds at HPHT conditions. *Colloids Surf. A Physicochem. Eng. Asp.* 2018; **537**; 361-71.
[19] S Medhi, S Chowdhury, JS Sangwai and DK Gupta. Effect of Al_2O_3 nanoparticle on viscoelastic and filtration properties of a salt-polymer-based drilling fluid. *Energ. Sources A Recovery Util. Environ. Eff.* 2019. https://doi.org/10.1080/15567036.2019.1662140
[20] S Medhi, S Chowdhury, DK Gupta and A Mazumdar. An investigation on the effects of silica and copper oxide nanoparticles on rheological and fluid loss property of drilling fluids. *J. Pet. Explor. Prod. Tech.* 2020; **10**, 91-101.
[21] O Mahmoud, A Mady, AS Dahab and A Aftab. Al_2O_3 and CuO nanoparticles as promising additives to improve the properties of KCl-polymer mud: An experimental investigation. *Can. J. Chem. Eng.* 2022; **100**, 1384-97.
[22] S Ponmani, R Nagarajan and JS Sangwai. Effect of nanofluids of CuO and ZnO in polyethylene glycol and polyvinylpyrrolidone on the thermal, electrical, and filtration-loss properties of water-based drilling fluids. *SPE J.* 2016; **21**, 405-15.
[23] A Aftab, AR Ismail, S Khokhar and ZH Ibupoto. Novel zinc oxide nanoparticles deposited acrylamide composite used for enhancing the performance of water-based drilling fluids at elevated temperature conditions. *J. Pet. Sci. Eng.* 2016; **146**, 1142-57.
[24] PAL Anawe and A Folayan. Investigation of the effect of yttrium oxide (y_2O_3) nanoparticle on the rheological properties of water based mud under high pressure high temperature (HPHT) environment. *Int. J. Mech. Eng. Tech.* 2018; **9**, 545-59.
[25] DV Kosynkin, G Ceriotti, KC Wilson, JR Lomeda, JT Scorsone, AD Patel, JE Friedheim and JM Tour. Graphene oxide as a high-performance fluid-loss-control additive in water-based drilling fluids. *ACS Appl. Mater. Interfac.* 2012; **4**, 222-7.
[26] J Aramendiz, A Imqam and SM Fakher. Design and evaluation of a water-based drilling fluid formulation using SiO_2 and graphene oxide nanoparticles for unconventional shales. *In*: Proceedings of the International Petroleum Technology Conference, Beijing, China. 2019.
[27] NM Taha and S Lee. Nano graphene application improving drilling fluids performance. In: Proceedings of the International Petroleum Technology Conference, Doha, Qatar. 2015.
[28] CY Ho, S Yusup and CV Soon. Study on the effect of nanoparticle loadings in base fluids for improvement of drilling fluid properties. *J. Adv. Chem. Eng*. 2014; **4**, 000115.
[29] AR Ismail, NM Rashid, MA Jaafar, WRW Sulaiman and NA Buang. Effect of nanomaterial on the rheology of drilling fluids. *J. Appl. Sci.* 2014; **14**, 1192-7.

[30] J Abdo and M Haneef. Nano-enhanced drilling fluids: Pioneering approach to overcome uncompromising drilling problems. *J. Energ. Resour. Tech.* 2012; **134**, 014501.
[31] A Aftab, AR Ismail and ZH Ibupoto. Enhancing the rheological properties and shale inhibition behavior of water-based mud using nanosilica, multi-walled carbon nanotube and graphene nanoplatelet. *Egypt. J. Pet.* 2017; **26**, 291-9.
[32] HM Ahmad, MS Kamal, M Mahmoud, SMS Hussain, M Abouelresh and MA Al-Harthi. Organophilic clay-based drilling fluids for mitigation of unconventional shale reservoirs instability and formation damage. *J. Energ. Resour. Tech.* 2019; **141**, 09310.
[33] S Elkatatny, M Mahmoud and HA Nasr-El-Din. Filter cake properties of water-based drilling fluids under static and dynamic conditions using computed tomography scan. *J. Energ. Resour. Tech.* 2013; **135**, 042201.
[34] O Mahmoud, HA Nasr-El-Din, Z Vryzas and VC Kelessidis. Effect of ferric oxide nanoparticles on the properties of filter cake formed by calcium bentonite-based drilling muds. *SPE Drill. Compl.* 2018; **33**, 363-76.
[35] O Mahmoud and HA Nasr-El-Din. Formation-damage assessment and filter-cake characterization of Ca-bentonite fluids enhanced with nanoparticles. *SPE Drill. Compl.* 2021; **36**, 75-87.
[36] AM Salem, MS Yakoot and O Mahmoud. A novel machine learning model for autonomous analysis and diagnosis of well integrity failures in artificial-lift production systems. *Adv. Geo-Energ. Res.* 2022; **6**, 123-42.
[37] WK Abdelbasset, SM Alrawaili, SH Elsayed, T Diana, S Ghazali, BF Felemban, M Zawawi, M Algarani, CH Su, HC Nguyen and O Mahmoud. Optimization of heterogeneous catalyst-assisted fatty acid methyl esters biodiesel production from soybean oil with different machine learning methods. *Arab. J. Chem.* 2022; **15**, 103915.
[38] OE Agwu, JU Akpabio, ME Ekpenyong, UG Inyang, DE Asuquo, IJ Eyoh and OS Adeoye. A critical review of drilling mud rheological models. *J. Pet. Sci. Eng.* 2021; **203**; 108659.
[39] S Gomaa, R Emara, O Mahmoud and AN El-hoshoudy. New correlations to calculate vertical sweep efficiency in oil reservoirs using nonlinear multiple regression and artificial neural network. *J. King Saud Univ. Eng. Sci.* 2022; **34**, 368-75.
[40] AM Salem, MS Yakoot and O Mahmoud. Addressing diverse petroleum industry problems using machine learning techniques: literary methodology-spotlight on predicting well integrity failures. *ACS Omega* 2022; **7**, 2504-19.
[41] M Nour, MS Farahat and O Mahmoud. Picking the optimum directional drilling technology (RSS vs PDM): A machine learning-based model. *In*: Proceedings of the ASME 41st International Conference on Offshore Mechanics and Arctic Engineering, Hamburg, Germany. 2022.
[42] OE Agwu, JU Akpabio, SB Alabi and A Dosunmu. Artificial intelligence techniques and their applications in drilling fluid engineering: A review. *J. Pet. Sci. Eng.* 2018; **167**, 300-15.
[43] S Elkatatny, Z Tariq and M Mahmoud. Real time prediction of drilling fluid rheological properties using artificial neural networks visible mathematical model (white box). *J. Pet. Sci. Eng.* 2016; **146**, 1202-10.
[44] K Abdelgawad, S Elkatatny, T Moussa, M Mahmoud and S Patil. Real-time determination of rheological properties of spud drilling fluids using a hybrid artificial intelligence technique. *J. Energ. Resour. Tech.* 2019; **141**, 032908.
[45] A Gowida, S Elkatatny, K Abdelgawad and R Gajbhiye. Newly developed correlations to predict the rheological parameters of high-bentonite drilling fluid using neural networks. *Sensors* 2020; **20**, 2787.
[46] A Golsefatan and K Shahbazi. A comprehensive modeling in predicting the effect of various nanoparticles on filtration volume of water-based drilling fluids. *J. Pet. Explor. Prod. Tech.* 2019; **10**, 859-70.
[47] M Gasser, O Mahmoud, F Ibrahim and M Abadir. Using artificial intelligence techniques in modeling and predicting the rheological behavior of nano-based drilling fluids. *In*: Proceedings of the ASME 40th International Virtual Conference on Ocean, Offshore and Arctic Engineering. New York, United States. 2021.
[48] MH Jondahl and H Viumdal. Estimating rheological properties of non-Newtonian drilling fluids using ultrasonic-through-transmission combined with machine learning methods. *In*: Proceedings of the IEEE International Ultrasonics Symposium, Kobe, Japan. 2018.
[49] OE Agwu, JU Akpabio and A Dosunmu. Artificial neural network model for predicting the density of oil-based muds in high-temperature, high-pressure wells. *J. Pet. Explor. Prod. Tech.* 2020; **10**, 1081-95.
[50] Z Abdelgawad, M Elzenary, S Elkatatny, M Mahmoud, A Abdulraheem and S Patil. New approach

to evaluate the equivalent circulating density (ECD) using artificial intelligence techniques. *J. Pet. Explor. Prod. Tech.* 2019; **9**, 1569-78.

[51] R Put, C Perrin, F Questier, D Coomans, D L Massart and Y V Heyden. Classification and regression tree analysis for molecular descriptor selection and retention prediction in chromatographic quantitative structure–retention relationship studies. *J. Chromatogr. A* 2023; **988**, 261-76.

[52] F Bre, JM Gimenez and VD Fachinotti. Prediction of wind pressure coefficients on building surfaces using artificial neural networks. *Energ. Build*. 2018; **158**, 1429-41.

[53] GE Hint. How neural networks learn from experience. *Sci. Am.* 1992; **267**, 144-51.

Appendix A

Table A1 Weight and bias for Eq. 3 rows (1 - 23) and columns (1 - 9).

i	W_{Ij}								
	j = 1	***j = 2***	***j = 3***	***j = 4***	***j = 5***	***j = 6***	***j = 7***	***j = 8***	***j = 9***
1	−0.64778	−0.3099	−0.48653	1.229989	0.606968	1.989165	−0.38779	−0.72041	−0.45034
2	−0.86945	0.664532	−0.27411	0.130968	0.075344	−0.30682	0.21268	−1.24793	0.340325
3	−0.77353	0.136169	1.338518	0.202651	−0.48534	0.843466	1.159328	−0.87146	0.468116
4	−1.18246	0.246263	0.316069	0.572225	0.515592	0.311262	−2.18585	−0.50918	−0.26433
5	0.92443	1.051067	−1.14065	−0.94434	1.277426	0.315198	1.694988	−0.32269	−0.92118
6	0.191732	−0.61927	0.304503	0.576718	0.636042	−0.10108	0.184795	−0.12359	−0.02483
7	0.039461	−0.5724	−0.17194	−2.63971	−0.97908	0.431412	0.442732	0.908695	0.54666
8	−0.1542	−0.19627	−0.58542	0.255135	−0.63668	−0.81467	−0.57777	−0.41554	0.174323
9	−0.79755	0.720688	−0.09105	−0.77653	−0.3226	−0.56603	0.839821	−0.27823	−0.34194
10	−0.8826	−0.47008	1.090779	0.030947	−0.48889	−0.44731	1.150097	−0.58407	1.187485
11	−0.59707	0.709758	0.710938	−0.43027	0.81805	0.325439	0.180943	−2.65786	0.681397
12	−0.49106	0.380776	0.727655	−0.98457	0.740415	−1.02164	−0.67419	−1.90E-01	0.023272
13	−0.18909	0.970757	0.002653	−1.92043	−0.31935	−0.69643	2.247897	0.098524	−0.25017
14	−0.56057	−0.20097	−0.44417	−0.02129	-0.52659	0.827392	−0.13272	−0.33405	0.618698
15	0.140978	−0.3958	0.154251	−1.53607	1.719036	1.372094	−0.21264	−1.00882	−0.2675
16	−0.68016	−0.61605	−0.26486	0.412975	1.096302	−0.23242	−0.35808	0.097963	0.170677
17	0.243923	−0.8613	0.590762	−0.144	−0.34957	−0.09262	0.901339	−1.09256	−0.4375
18	−0.53319	1.350096	0.853673	0.741228	−1.06728	0.922307	0.752868	0.955811	0.643999
19	0.845794	0.60739	−1.00476	0.852502	−1.30714	0.087136	−1.04482	0.407896	−0.42785
20	−0.02439	0.372009	0.195756	−0.90934	2.417362	−0.55115	−1.31099	0.628244	−0.44805
21	0.447819	1.019972	−1.36653	−0.14091	−0.18558	0.151587	0.163731	1.069158	0.261992
22	0.717982	0.219749	−0.41631	−0.25417	−0.84213	0.519928	0.384458	−0.06271	0.449732
23	−0.19658	0.262977	−0.72244	−0.22291	1.020478	0.212464	−0.95081	1.11238	-0.42187

Table A2 Weight and bias for Eq. 3 rows (24 - 46) and columns (1 - 9).

i	W_{Ij}								
	j = 1	***j = 2***	***j = 3***	***j = 4***	***j = 5***	***j = 6***	***j = 7***	***j = 8***	***j = 9***
24	0.539811	−0.53835	−0.81006	−0.39887	1.302577	−0.97235	−0.29503	−0.37828	0.570461
25	−0.29628	−0.46217	0.183049	−0.96719	−0.3192	−0.05161	−0.80898	−0.50843	−0.39156
26	0.292517	−1.69298	1.15685	−0.66949	−0.1451	−0.20199	0.465459	−0.36158	−0.29948
27	−0.35159	0.378334	−0.65571	−0.34042	−0.67033	−0.58948	−1.0611	2.228297	1.346806
28	−0.22103	1.118151	−0.58258	0.891583	0.354337	−0.39731	0.184497	0.264171	0.664258
29	−0.15293	−0.72933	−0.25695	0.635614	0.700274	0.466619	0.263811	0.652755	−0.05399
30	1.111865	−0.27416	−0.77326	0.299911	1.258009	0.507211	−0.33843	1.130111	−0.22248
31	0.393409	−0.40842	−0.01655	−0.24866	0.871338	0.728062	−2.04146	0.298034	0.142678
32	−1.22802	0.777846	−1.67592	0.117299	0.26519	−0.07687	−0.65342	0.613856	0.375737
33	1.550207	−1.51902	−1.26669	−0.69959	2.800572	0.074432	0.036828	−0.03131	−0.50332
34	−0.17562	0.256634	−0.21193	0.072232	−0.88952	−0.0412	0.152038	−0.02341	0.38647
35	0.598268	0.672578	−1.07321	−0.94309	0.634317	−0.53269	0.364349	0.155688	0.494331
36	0.904676	0.240262	−0.1085	−0.82088	−0.1909	0.366673	0.344198	−0.52414	−0.13471
37	−0.26114	−1.16473	−0.65075	1.946204	−0.22003	0.439237	−0.55896	−0.17676	−0.02198
38	−0.52442	−0.36311	−0.33274	−0.73224	−1.65193	−0.4077	−0.17722	0.353911	−0.33135
39	−0.01005	−0.24413	−0.33128	2.428993	−0.30053	−1.19985	−0.30199	−1.47104	−0.27132
40	−0.73978	−0.39221	0.426648	−0.5811	−2.43494	−1.28531	−0.3601	−0.29053	−0.01145
41	2.604756	2.560748	2.415438	0.312403	0.019277	0.263348	0.484124	0.284521	−0.01191
42	0.044142	1.497931	−0.37249	0.316169	−1.77984	0.929333	−0.19184	−0.30822	−0.17502
43	0.305512	−0.67663	−1.28739	0.739684	−0.44816	−0.24677	−0.09696	−0.1351	−0.07242
44	−0.65174	−0.74562	0.937129	0.185005	0.130262	2.251297	−0.32495	−1.10818	0.614193
45	0.276272	0.384989	−0.27063	−0.6475	0.843202	−1.54329	0.511008	0.262442	0.077479
46	0.170226	0.821096	−0.29167	−1.0784	−1.04471	0.132506	0.287534	1.207685	0.170626

Table A3 Weight and bias for Eq. 3 rows (1 - 23) and columns (10 - 18).

i	W_{1j}						W_{2i}	b_1	b_2
	j = 10	**j = 11**	**j = 12**	**j = 13**	**j = 14**	**j = 15**			
1	−0.34226	−0.44584	−0.9539	−0.62197	−0.68682	0.668817	2.08248	1.921287	
2	−0.67702	−0.6737	−0.30653	0.921253	−0.55096	−0.78819	1.342997	1.554237	
3	0.859592	−1.13364	−0.88554	0.187966	0.403091	−0.29543	−2.00902	1.447229	
4	1.142522	0.368905	0.294332	0.541771	0.045076	−0.09197	−1.25849	1.543998	
5	−0.68704	1.154577	−1.42153	−0.86872	−0.76976	0.237965	−2.0634	−1.0265	
6	−0.64902	−0.51238	−0.60513	0.648028	0.421773	0.110586	0.326823	−1.48313	
7	1.026893	0.870988	−0.6611	−1.049	−0.19452	−2.51094	0.774512	1.040371	
8	−0.65708	−0.574	−0.45438	−0.38212	0.297756	0.102583	−0.49151	1.258612	
9	−0.61448	0.972945	−0.10405	0.244656	0.631054	−0.88493	0.942088	1.308099	
10	−2.18184	−0.75838	−0.55639	0.459221	1.257107	0.164349	1.185106	1.290668	
11	−2.02776	−0.54684	−0.82366	−0.85301	−0.96951	−0.34907	−1.42671	0.835465	
12	0.787044	−0.74812	0.729189	0.213805	1.095762	1.343766	−1.11951	−0.23666	−1.34957
13	0.75698	0.717647	−0.04438	−0.97463	−0.05028	−1.15826	−1.51123	−0.94862	
14	−0.05068	−0.45199	0.570728	−0.67065	−0.4596	0.159244	0.003258	0.79001	
15	0.867984	−5.33139	1.080313	0.22264	2.626737	0.113129	1.875133	0.845903	
16	0.391442	−0.1188	0.674819	−0.03685	0.408585	1.278477	1.211438	0.303829	
17	−0.5977	−0.40903	−0.02692	1.264747	−1.3782	0.721703	1.658309	0.32931	
18	1.092927	−0.80562	−1.02899	0.837289	0.800846	−2.65876	2.420331	−1.37566	
19	1.070429	−0.04333	−0.42192	−1.56936	−0.28342	0.226603	−1.80663	−0.01805	
20	−0.49975	2.883887	−1.05733	−0.29392	−0.54265	−0.16876	1.874048	0.143122	
21	1.196574	0.32413	0.741051	−0.0857	−1.30482	0.533793	1.640258	0.435205	
22	0.584451	0.124875	0.037035	−0.59466	0.41246	−1.15828	0.821334	−0.43684	
23	0.235196	−0.38751	−1.46811	−0.15235	0.770721	−0.02756	1.610283	0.165496	

Table A4 Weight and bias for Eq. 3 rows (24 - 46) and columns (10 - 18).

i	W_{1j}						W_{2i}	b_1	b_2
	j = 10	*j = 11*	*j = 12*	*j = 13*	*j = 14*	*j = 15*			
24	−0.66296	0.86749	−1.0414	−0.35602	1.152689	1.347839	−0.68496	0.696289	
25	−0.24502	0.442304	−0.91912	−1.18027	0.077182	1.423942	−1.48818	6.56E-05	
26	−0.04242	−0.13204	0.076173	0.131812	−0.18449	−3.34212	−0.90046	−0.93137	
27	0.195415	−1.5189	−0.25502	0.354177	−0.64836	0.017978	−0.80867	0.125339	
28	−0.39884	−0.92162	−1.76659	1.117921	−1.12788	−1.24749	−1.49801	−0.48353	
29	0.186601	0.476103	0.00247	0.920847	−0.07564	0.327881	1.312972	−0.69701	
30	0.449197	−1.60535	−0.30534	0.536013	0.5598	0.050234	−1.61589	0.603635	
31	0.214522	0.875384	0.196536	1.196888	−0.7226	1.018956	−1.68696	0.777364	
32	−0.21619	0.685055	−0.96776	0.245557	1.323715	2.430727	−1.08527	0.743644	
33	−2.02197	−0.13452	−0.03015	0.022681	0.339171	0.400377	−1.90212	1.50391	
34	0.849608	0.600135	0.856123	−0.15916	−1.1494	−1.07914	1.291217	−1.31654	
35	−1.0642	3.42599	−1.81906	−0.56658	−0.14011	0.473204	2.678062	0.917696	
36	−1.18607	0.651502	0.466215	−0.07565	−0.00287	0.431553	−1.27658	1.115086	
37	−0.32325	−0.7934	0.659888	−0.54019	2.071558	−2.81961	−0.54194	−1.2481	
38	0.727123	0.24196	−0.5485	0.353569	0.474749	1.698317	0.845593	−1.46551	
39	0.058422	1.04844	−1.88542	0.105403	2.29295	−1.78081	1.335647	−1.29143	
40	−0.20841	−0.35436	−0.82182	1.070256	−0.28262	1.147051	−1.17171	−1.19634	
41	0.058703	−0.53912	−0.03205	0.242032	−0.84892	−10.724	−4.7534	−9.31856	
42	0.539454	0.357257	1.42061	0.114877	0.218042	−1.0537	−1.58678	−1.62512	
43	0.148645	0.223123	−1.46275	0.325126	−0.26438	0.322854	−0.77976	−1.45794	
44	−0.39625	0.31129	−0.56985	0.112519	−0.21833	−0.45633	−1.15149	−1.58305	
45	−0.2583	0.93565	0.722895	0.123258	0.446731	−0.082	−1.18378	1.812632	
46	0.709475	0.137969	0.952679	−0.41863	0.094847	1.346704	0.945589	2.277298	